Effect of post welding heat treatment on the weld quality of micro plasma arc welded SS-316L thin sheet

Srikant Prasad[1] , Sukhomay Pal[1] , P. S. Robi[1]

[1] Indian Institute of Technology Guwahati, Department of Mechanical Engineering, Guwahati, Assam, India.

Abstract: High thermal gradient formed during the fusion welding process results in development of undesirable residual stress in the weldments. This stress is developed due to restraint by the parent metal during weld solidification. The high heat input results in non-uniform heat distribution across the weld region in other words non-uniform microstructural development across the weld region and hence the mechanical properties of the joint are often not uniform. In order to avoid inhomogeneity in the mechanical properties and also to reduce/eliminate undesirable residual stress, the welded samples are given post welding heat treatment. In this research, 500 µm thin SS-316L sheets are welded using micro plasma arc welding process and then the welded specimens are heat treated. The welding experiments are conducted by varying welding speed, welding current and stand-off distance. Weld bead microstructure, micro-hardness, ultimate tensile strength (UTS), yield strength and percentage elongation are determined before and after heat treatment. The effects of welding heat input and process parameters on the measured weld qualities are studied. Analysis of variance is also performed to estimate the influence of factors and their interaction on the weld quality. The post weld heat treatment results in an increase in the grain size of the HAZ and is found in the range of 38.96 µm to 56.22 µm whereas for as-welded samples it is in the range of 29.88 µm to 50.40 µm. The average UTS value of the heat treated samples is increased by 9.9% compared to the as-welded samples. The hardness of the fusion zone varies in the range of 175-215 HV.

Key-words: Plasma arc welding; Heat treatment; Tensile properties; Microstructure; Analysis of variance; Regression model; SS-316L.

1. Introduction

Thin stainless steel sheets are extensively used in automobile, aerospace, ship building and sport industries because of its superior mechanical properties at cryogenic and elevated temperature, better corrosion resistance and creep resistance [1]. The use of thin section can significantly reduce the vehicles' weight that helps to minimize the fuel consumptions and carbon dioxide emissions, which is of great concern nowadays. Welding is a vital assembling technique used in many industries and plays a significant role in determining the final strength of the product. The challenges encountered during thin sheet welding are generally linked with heat input. Uncontrolled and excessive heat offered by the conventional tungsten inert gas and metal inert gas welding processes leads to burn through, distortion, buckling, twisting and joint gap variation during welding [2]. To overcome the adverse effects of high heat input, controlled and small heat input through laser or electron beam welding processes have been investigated. These welding processes offer many advantages including minimal weld distortion, high seam quality and high welding speed with higher energy efficiency for joining thin sheets [3]. However, the use of these welding processes is limited to large industries due to the exorbitant equipment cost. Most of researchers work on laser or electron bean welding for thin sheet but in this research our objective is to obtain desirable quality by micro plasma arc welding (MPAW) process for same thin stainless steel sheet.

The MPAW technique appears to be a better choice for many joining applications due to high weld quality, better arc stability, low current arc stiffness and less sensitive to arc length variation than TIG welding [1,4] and lower equipment cost compared to electron and laser beam welding processes. In addition, it has high tolerance to joint misalignment compared to laser or electron beam welding. Previous studies showed that process parameters have significant effect on the weld bead geometry of SS-304L [5-7], AISI 316 [8], AISI 316L [9] mild steel [10], 2205 duplex steel [11]. However Yoshioka et al. [12] found that stand-off distance does not have much effect on the weld quality of 0.1 mm and 0.3 mm thick SS-304 sheets. The tensile property of MPA welded SS-304L [5] and SS-316L [13] sheets were also studied. The weldment strength, hardness, impact resistance, corrosion resistance and hot-cracking susceptibility fully depends on microstructure and solidification behavior of the fusion zone [14,15]. The mechanical properties of the austenitic stainless steel joints significantly decrease due to formation of dendritic structure, presence of hard phases, high elemental segregation and nonhomogeneous microstructure in the

weldment [14,16]. In order to modify and improve the microstructure of the weldment, grain refinement by post weld heat treatment can be adapted.

The post welding heat treatment results in almost homogeneous microstructure and facilitates removal of metallurgical defects like dislocations, vacancies and slip planes and also removes residual stresses formed during the welding process. Another important aspect of heat treatment is that it reduces the brittle fracture of the weldment. Hence, the study of post welding heat treatment on the microstructure and mechanical properties of the SS 316L sheets is also important for its useful application. Some researchers reported the effect of post welding heat treatment on mechanical and microstructural properties of austenitic, martensitic and duplex strain less steel welds [17-27]. Kose and Kacar [17] studied the effects of pre- and post-welding heat treatments on the microstructure and mechanical properties of CO_2 laser welded AISI 420 weldments. Improved mechanical properties were observed due to heat treatments. Liu et al. [18] studied the effect of post welding heat treatment on the creep fatigue resistance of TIG welded SS-308L weldments. The as-welded samples of P92 material joint by TIG welding process showed heterogeneous microstructure whereas, after heat treatment the heterogeneity reduced to a great extent [19]. Bal et al. [20] found that all the as-welded Hastelloy C-276 sheets joint by laser welding process failed at the weld zone. However after post welding heat treatment, the samples which were welded with heat input of 120 J/mm, failed at the base metal. Du et al. [21] obtained 600 °C as optimum temperature for post welding heat treatment of laser welded dissimilar joint of 2205DSS and Q235. At this heat treatment temperature highest toughness of the weldment was observed. Xin et al. [22] welded 316LN steel plates using multi-pass TIG welding process. They found that post welding heat treatment temperature has marginal effect on the UTS values but percentage elongation of the weldment increased with annealing treatment. Jang et al. [23] performed post welding heat treatment of SS304 weldment and found superior mechanical property, compared to the as-welded samples, due to the decrease of the δ-ferrite and the recrystallization of the austenite structure. Barbosa Gonçalves et al. [24] studied the microstructure of AISI-347 austenitic steel weldment. The result exhibited grain growth in the HAZ after conventional solution and stabilizing heat treatment compared to as-welded samples. Gonzaga et al. [25] welded AISI 347 austenitic steel pipes using hot wire tungsten inert gas welding and studied the microstructure and corrosion resistance of post welding heat treated samples. The microstructure of post weld ageing sample revealed sensitization in the HAZ/FZ/BM interfaces. Tyson [26] reported enhanced UTS by post welding heat treatment of 316L and 347 austenite stainless steel weldments. Hamada and Yamauchi [27] used post welding heat treatment for relieving of residual stress of austenitic stainless steel weldment.

Although MPAW process has been investigated successfully for welding stainless steel, there is not much recent work on MPAW of SS-316L sheet. Moreover, there are no studies on effect of post welding heat treatment of MPAWed SS-316 weldments. Therefore in this research, a detailed investigation is carried out to evaluate the effect of post welding heat treatment on the weld properties of SS-316L weldments. Weld bead microstructure, micro-hardness and mechanical properties (ultimate tensile strength, yield strength and percentage elongation) are determined for the as-welded and heat treated samples. The effects of welding heat input and process parameters on the measured weld qualities of heat treated weldments are studied. Analysis of variance (ANOVA) is also performed to estimate the influence of factors and their interaction on the weld quality.

2. Experimental Procedure and Results

The difficulty of joining thin sheets using fusion welding process increases with decrease in the material thickness. The challenges such as joint gap variation, edges mismatch and position of the welding torch with respect to the joint line become more significant. Therefore, suitable jig & fixture is essential for successful welding of thin sheet using MPAW process. A customized setup has been designed to align the plasma torch along the weld line and to control the stand-off distance (SOD) precisely during welding. The welding machine used for the study is ARCRAFT Plasma Equipment's Pvt. Ltd. make semi-automatic digital micro plasma welding machine (Model: MP-50). A tungsten electrode with tip angle of 20° and diameter of 1.2 mm was used along with 1.2 mm diameter copper nozzle. Argon gas was used as both plasma and shielding gas at a flow rate of 2 liter per minute. The welding speed was controlled by a motor driven carriage with a variable speed in the range of 1 mm/s to 10 mm/s. Two rolled SS-316L sheets of 500 μm thickness, 150 mm length and 50 mm width were welded perpendicular to the rolling direction in single side square butt joint configuration along the length. The measured chemical composition, in weight percentage, of the workpiece material is: C-0.03, Mn-1.1, Si-0.5, P-0.1, S-0.1, Mo-1.9, Cr-17.4, Ni-10.4, Fe - 68.47. The measured ultimate tensile stress (UTS), yield stress (YS), percentage elongation (EL) and micro-hardness of the as-received work piece material are 720 MPa, 339 MPa, 74.05% and 168 HV, respectively.

A feasibility study was performed by varying welding speed within 2.7 – 5.7 mm/s and welding current 4 – 12 A, keeping all other parameters constant, to identify parametric ranges for successful joining. Good welding with full penetration was found within 8 – 11 A welding current. Partial welding and heating were observed below 8 A current whereas above 11 A current workpiece materials melted and holes were made. Partial penetration was also observed at high welding speed. Satisfactory welding was noticed in the range of 2.7 – 4.7 mm/s welding speed and 8 – 11 A welding current. Therefore, with these feasibility ranges and information from the published literature, a three factors, three/four mixed levels full factorial design matrix was developed and main experimental runs were carried out as per Table 1. Four levels were considered for welding current and

three levels for each welding speed and SOD. After completion of welding experiments, samples were extracted to measure as-welded mechanical properties, micro-hardness and microstructure. Samples were also extracted for post welding heat treatment operation.

Table 1. Design matrix of full factorial design.

	Process parameters		
Exp. No.	Welding current (A)	Welding speed (mm/s)	Stand-off distance (mm)
1	8	2.7	1
2	8	3.7	1
3	8	4.7	1
4	9	2.7	1
5	9	3.7	1
6	9	4.7	1
7	10	2.7	1
8	10	3.7	1
9	10	4.7	1
10	11	2.7	1
11	11	3.7	1
12	11	4.7	1
13	8	2.7	1.5
14	8	3.7	1.5
15	8	4.7	1.5
16	9	2.7	1.5
17	9	3.7	1.5
18	9	4.7	1.5
19	10	2.7	1.5
20	10	3.7	1.5
21	10	4.7	1.5
22	11	2.7	1.5
23	11	3.7	1.5
24	11	4.7	1.5
25	8	2.7	2
26	8	3.7	2
27	8	4.7	2
28	9	2.7	2
29	9	3.7	2
30	9	4.7	2
31	10	2.7	2
32	10	3.7	2
33	10	4.7	2
34	11	2.7	2
35	11	3.7	2
36	11	4.7	2

2.1. Post weld heat treatment procedure

The welded samples were kept in a resistance heated muffle furnace and heated to 1000 °C. The samples were then soaked at this temperature for 120 minutes and subsequently water quenched to room temperature. The post weld heat treatment cycle was decided based on the standard heat treatment cycle followed for the SS 316L [28]. Water quenching was followed to avoid the re-precipitation of chromium carbide which may occur during slow cooling in the temperature range 816 – 427 °C.

2.2. Micro-hardness measurement

A Vickers's micro hardness testing equipment (Make: Buehler, Model: Micromet-2101) with a square base pyramid shaped diamond indenter having 136° included angle was used for testing in the Vickers scale. The test is carried at 500 g load for 10 s dwell time. Test samples for measurement of micro-hardness in the weld bead (both for as-welded and post welding heat treated samples) were cut normal to the welding direction. Then the extracted specimens were polished using emery papers. In this work, micro-hardness values were measured at three different layers namely, top, middle and bottom layers, which are along the cross section of the specimens. A total of thirteen micro-hardness values were measured in each sample. For representation purpose photograph of a micro-hardness tested as-welded specimen is shown in Figure 1. In each specimen, five micro-hardness values (P1, P2, P3, P4 and P5) were measured in the middle layer of the fusion zone (FZ), one each in the top (P6) and bottom (P7) layers of the FZ. Six measurements were taken at the heat affected zone (HAZ), three in each side of the FZ.
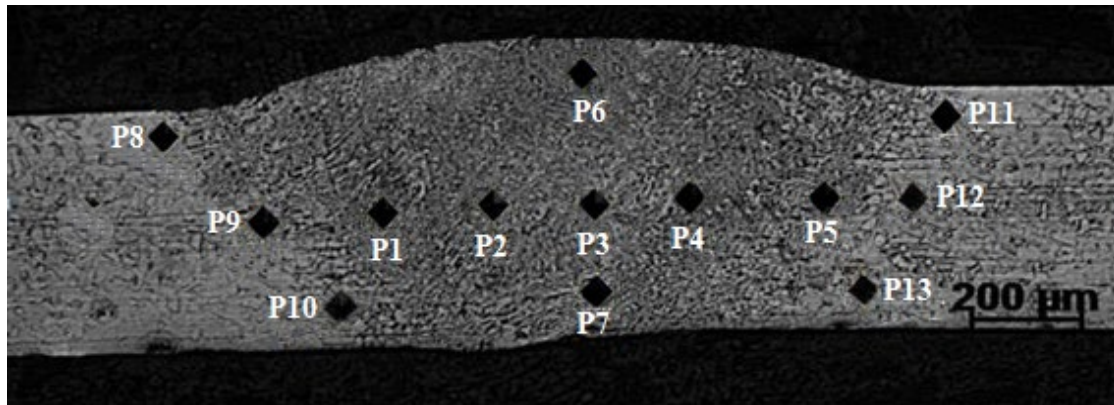
Figure 1. Photograph of a micro-hardness tested specimen with indentation marks (as-welded sample).

2.3. Weld bead microstructure

Test specimens for relevant microstructural examination were taken from as-welded and post-weld heat treated samples, in such a manner that it includes the FZ, HAZ and parent metal. The specimens were then prepared with standard metallographic specimen preparation technique for microstructural study. The microstructure of the weld region was observed under optical microscope (Make: Zeiss, Model: Axiotech) and the grain size of different zones were measured by line intercept method.

2.4. Tensile test

Universal tensile test was conducted to measure the ultimate tensile stress (UTS), 0.2% yield stress (YS) and percentage elongation (% EL) of the as-welded and post welding heat treated samples during static loading. For as-welded condition, three tensile test specimens are extracted from each welding specimen. Similarly, for post welding heat treatment condition, two specimens are extracted from each welding specimen. An extensometer with gauge length of 25 mm is used to measure the percentage of elongation. A hydraulically operated servo controlled universal testing machine (Make: Instron; Model: 8801) is used for the tensile testing with a constant speed of 1 mm/min and at room temperature.

3. Analysis of weld qualities

3.1. Analysis of weld bead microstructure

Few optical micrographs taken at various weld zones are shown in Figure 2 and Figure 3 for as-welded and heat treated welded samples, respectively. It can be seen in Figure 2 that the grains size at the FZ cannot be measured. The high rate of heat extraction resulted in extremely very fine grains in the as-welded FZ, the size of which could not be measured using optical microscope. However, the grain size at the HAZ and parent metal are measurable.

(a)

(b)

(c)

(d)

(e)
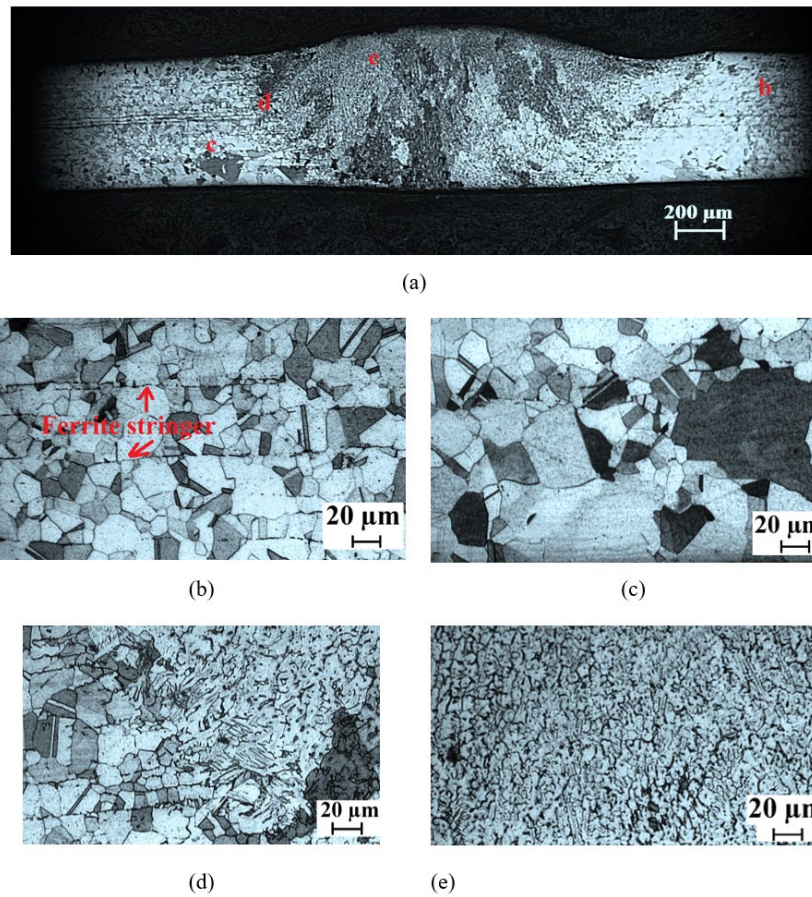
Figure 2. Microstructure of as-welded sample of Exp. No. 7, (a) full weld zone, (b) base metal, (c) heat affected zone, (d) interface of FZ and HAZ and (e) fusion zone.

(a)

(b)

(c)

(d)
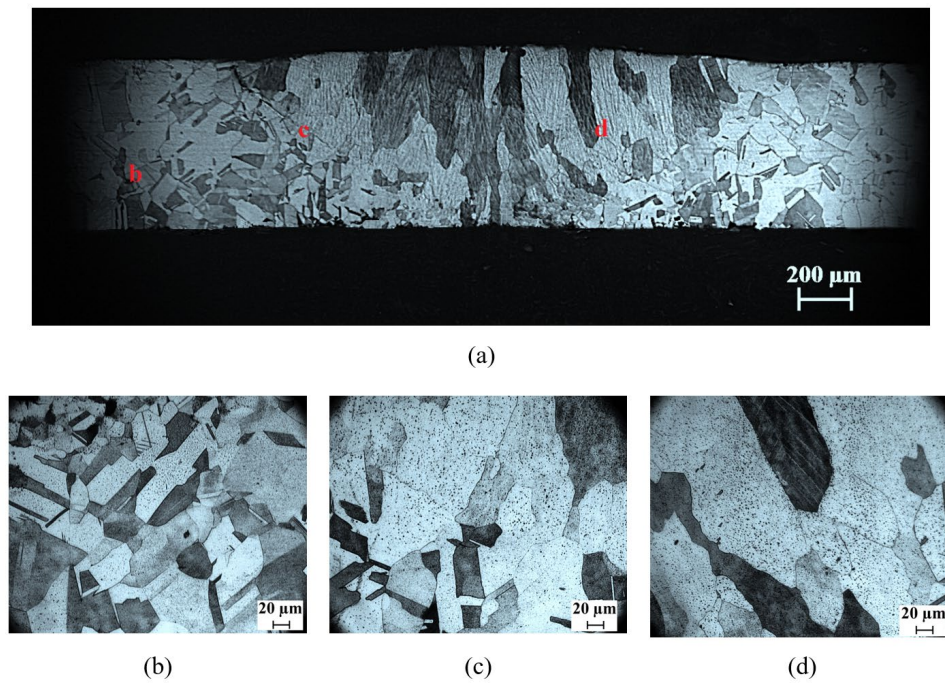
Figure 3. Microstructure of heat treated sample of Exp. No. 7, (a) full weld zone, (b) base metal region (c) interface of fusion zone and base metal and (d) fusion zone.

Typical microstructure of a welded sample after annealing is shown in Figure 3. The microstructure of the weld zone of the specimen shows only two regions: the fusion zone and base metal zone. The size of the grains in the fusion zone is coarse compared to that of the as-welded (Figure 2) samples. The HAZ is not observed in the microstructure of the weldments after annealing. As evident in Figure 2, HAZ is having fine grained structure in the as-welded specimen. During heat treatment, growth of the recrystallized grains at the HAZ of the welded sample took place and reached almost the same size as the grain size of the base metal. Hence a clear distinction between the base metal and fusion zone is evident in the annealed microstructure (Figure 3c). In all the as-welded samples, stringers of high temperature ferrite (δ-Fe) aligned along the rolling direction was observed (Figure 2b). The similar austenite and ferrite structure for SS-316L welded samples were also observation by Silva et al. [29] and Sánchez-Tovar et al. [30]. However, stringers of high temperature ferrite (δ-Fe) are not observed after heat treatment (Figure 3). This is due to the fact that during annealing process, almost all δ-ferrite stringers, which were formed during the welding process, transforms to austenite under equilibrium cooling conditions [31]. Heat treatment of the sample resulted in eliminating the HAZ as well as the ferrite stringers formed during welding.

3.1.1. Effect of heat input on grain size of heat treated weldments

The amount of base material melt during MPAW process depends upon the heat input which in turn governs the weld microstructure and mechanical properties. The welding heat input per unit length of the workpiece is calculated using Equation 1.

$$\text{Heat input per unit length} = \frac{V \times I}{WS} \qquad (1)$$

where, V is welding voltage in volt, I is welding current in ampere and WS is the welding speed in mm/s. Figure 4 depicts the variation of grain diameter with welding heat input before and after heat treatment. The grain size of as-welded samples varies in the range 17.1 μm to 28.8 μm. It also shows an increasing trend with increase in welding heat input. With increase in heat input the amount of energy dissipated in the material increases resulting in recrystallization and grain growth and hence an increase in the grain size. Heat treatment results in an increase in the grain size of the welded sample and is found to be in the range of 38.96 μm to 56.22 μm. However no trend in the grain diameter with heat input is observed in the heat treated samples. During welding unstable microstructural changes due to high heat input and fast cooling rate takes place resulting in internal stresses around the welded region. These are regions where initiation of metallurgical phenomena like nucleation / grain growth can occur. During annealing heat treatment the nucleation / grain growth takes place at a faster rate resulting in relieving of internal stresses and subsequent growth of the nucleated grains. This nullifies most of the detrimental effect of heat input on the weldment. However, the result (Figure 4) indicates a higher scatter in the grain size of heat treated samples. There is a large scatter in the grain size for heat input less than around 80 J/mm (38.96 μm to 55.71 μm). For heat input beyond 83 J/mm, the grain diameter variation is less and varies within 40.61 μm to 48.45 μm, except in one case. This variation in the grain diameter is acceptable for all practical purpose.

Partial weld penetration is observed in samples with welding heat input less than 80 J/mm. In these cases, the energy dissipated during welding is less compared to the weldments with full penetration. The activation energy necessary for occurrence of the metallurgical phenomenon like grain growth is high. This leads to incomplete annealing process during heat treatment thereby resulting in larger scatter in the grain diameter. However, the same annealing process ensured almost same grain size for the samples with full weld penetration.
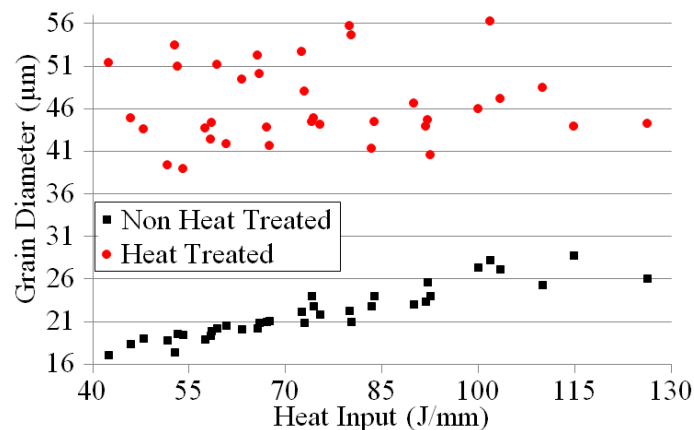
Figure 4 Variation of grain size at the HAZ with welding heat input.

3.1.2. Effect of process parameter on grain size of heat treated weldments

The variations in the grain diameter vs. process parameters for the heat treated weldments are plotted in Figure a-c. For a particular welding speed and stand-off distance, the welding current has no significant effect on the grain diameter. The grain diameter increases with increase in welding speed up to 3.7 mm/s for 10 out of 12 cases and with further increase in the welding speed the grain size decreases for 7 out of the 12 cases, as shown in Figure 5b. Similar result is observed with variation in stand-off distance. However, in case of as-welded samples, the grain diameter decreases with increasing welding speed as shown in Figure 5d. The heat input decreases with higher welding speed and stand-off distance resulting in incomplete weld penetration. This leads to the decrease in grain size at higher welding speed and sand-off distance.
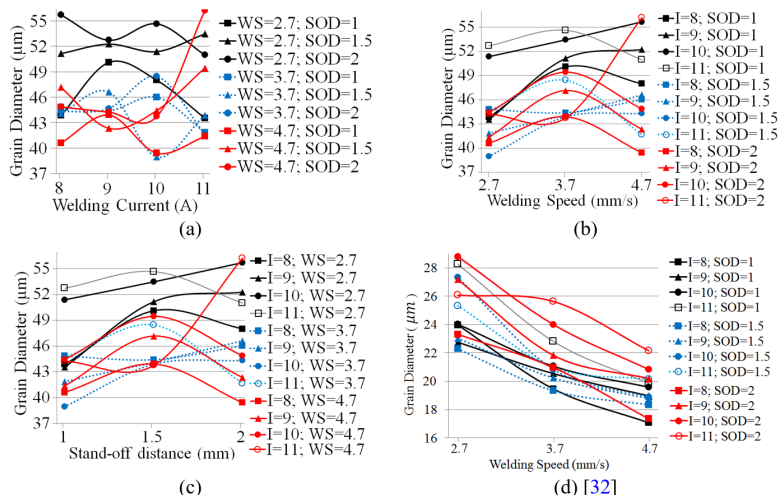
Figure 5. Variation of grain size at HAZ with (a) welding current (b) welding speed and (c) stand-off distance of heat treated samples (d) welding speed for as-welded samples [32].

3.1.3. Influence of process parameters on grain size

In section 3.1.2, it has been found that the variation of microstructure of HAZ in the weldments after heat treatment is not well correlated with individual process parameters, viz. welding speed, welding current, and stand-off distance. This may be due to the significant interaction effect of controllable parameters. Therefore, to study the effect of various factors and their interaction on the grain size, three-way ANOVA [33] is performed. The percentage contributions of each factor and interaction on the grain diameter of the heat treated weldments has been calculated and given in Table 2. It is found that the contribution of stand-off distance and welding speed are insignificant at 90% confidence level. The influence of interaction of stand-off distance and welding speed is highest with 26.8% contribution. However, the contribution of error is highest with 28.9%. This high error may be due to partial weld penetration. During annealing heat treatment, the nucleation / grain growth takes place. This nucleation / grain growth phenomenon occurs faster at regions of higher internal residual stresses especially at HAZ. The nucleation during annealing is always accompanied by relieving of internal residual stresses. The grain growth results in coarse grain structure leading to further reduction in residual stresses by means of reduction in surface energy. HAZ is always a region of higher energy compared to the other regions of the weldment. During annealing the faster grain growth at HAZ results in coarse grained structure and reaches the size comparable to that of the base metal. This is evident by comparing Figures 2 and 3. In Figure 2, HAZ is clearly visible whereas, in Figure 3 due to the grain growth the HAZ is not visible. Because of this the effect of process parameters on the grain size / microstructure of the heat treated samples are nullified and more or less homogeneous microstructure is obtained. The purpose of carrying out the heat treatment of the welded sample was to reduce the non-homogeneity in the microstructure. This is achieved by the heat treatment process.

Table 2. Percentage influence of process parameters on grain diameter.

Factor	I	WS	SOD	I×SOD	I×WS	SOD×WS	I×SOD×WS	Error
Percentage influence	7.0	4.5#	4.2#	---	9.1#	26.8	19.5#	28.9

effect of these parameters is insignificant at 90% confidence level.

3.1.4. Development of mathematical models

The relation between the MPAW process parameters and the grain diameter of post welding heat treated samples is examined using regression models. The regression models developed for grain size ($Grain\,Dia$) is as follows:

$$Grain\,Dia = 16 - 5.5I + 107.9(SOD) + 16.3(WS) + 1.15I^2 - 6.52(SOD)^2 + 2.1(WS)^2$$
$$- 3.69I(WS) - 10.1I(SOD) - 19.8(SOD)(WS) + 2.36I(SOD)(WS)$$

(2)

The ANOVA test result is shown in Table 3. From the table it is found that the regression model is inadequate at 95% confidence level. The value of correlation coefficients is just around 0.3. The reason for inadequate correlation of grain size with process parameters is mainly due to the fact that heat treatment nullified the effect of welding process parameters.

Table 3. ANOVA **table for** regression model of grain size.

Source	DOF	SOS	V	F-Value	P-Value	Whether the model is adequate
Grain Dia	10	230.619	23.062	1.09	0.407	**No**
Residual Error	25	529.510	21.18			
Total	35	760.128				

R^2 value: 30.34%. Adjusted R^2 value: 2.48%

3.2. Analysis of mechanical properties

After heat treatment, two tensile test specimens were extracted for each welding condition. The average values of UTS, YS and %EL were considered for analysis. The analyses of the results are as follows.

3.2.1. Effect of welding heat input on mechanical properties

The variation of UTS, YS and %EL vs. welding heat input is plotted in Figure 6a-c, respectively. The UTS, YS and %EL increases with increase in heat input. UTS of the heat treated weldments is higher than that of the as-welded samples for welding heat inputs up to 92 J/mm. Beyond 92 J/mm this properties is almost similar for the heat treated and as-welded samples. The %EL for the heat treated sample is higher than the as-welded samples up to a heat input of around 100 J/mm. Beyond this the %EL remains almost same with a deviation of 7.6%. Yield strength of the weldment decreases after heat treatment for 27 out of 36 cases. The reason for this trend is that incomplete penetration up to a heat input of 80 J/mm and beyond this it was full penetration. During heat treatment, the residual stresses and other metallurgical non-homogeneities were reduced [23,24,26] resulting in higher UTS and percentage elongation for the heat treated samples compared to as-welded samples.

(a)

(b)

(c)
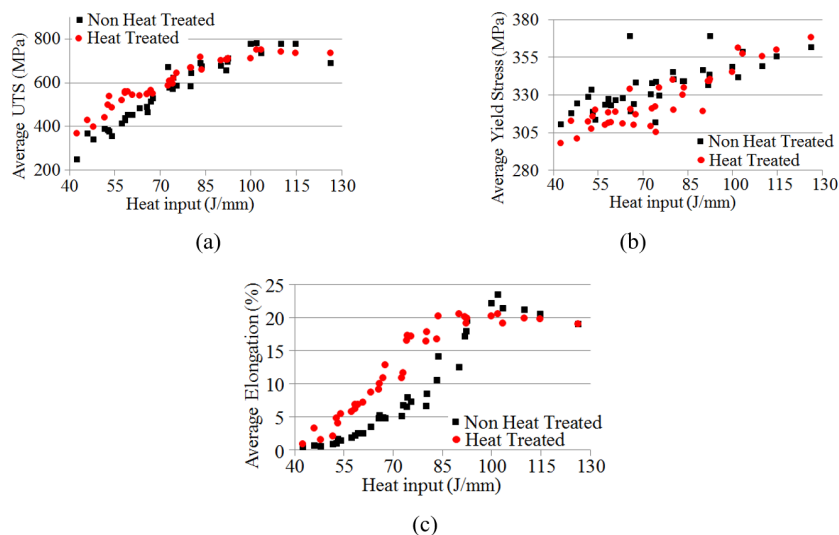
Figure 6. Variation of (a) ultilate tensile stress, (b) 0.2% yield stress and (c) % elongation.

3.2.2. Effect of process parameters on mechanical properties

Figure 7a-c shows the plots of UTS, YS and % EL values vs. welding current of heat treated samples. For a constant stand-off distance and welding speed the UTS and % EL show an increasing trend with increase in welding current. With increase in welding current, the heat input increases leading to full penetration thereby resulting in increased UTS and % elongation. The variation of UTS with welding current of as-welded samples is shown in Figure 7d, the plots of YS and % EL values vs. welding current of as-welded samples can be found in [32]. The trend is similar except the spread is larger.
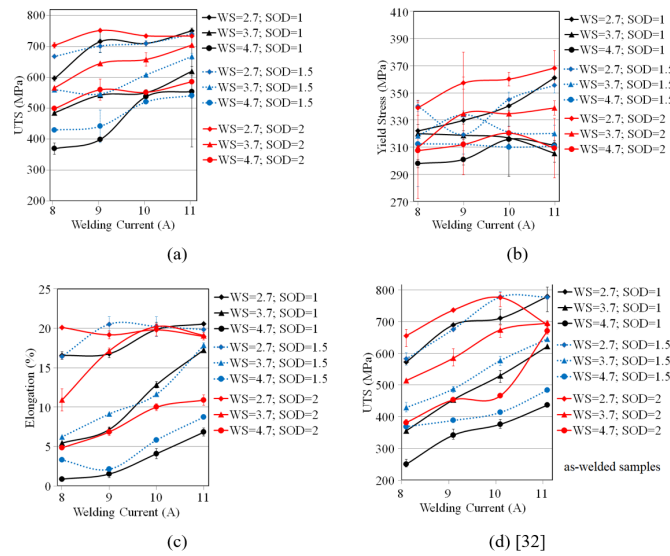
Figure 7. Variation of (a) UTS, (b) yield stress and (c) percentage elongation with welding current of heat treated samples (d) UTS with welding current for as-welded samples [32].

Figure 8a-c shows the plots of UTS, YS and % EL values vs. welding speed. For a constant welding current and stand-off distance, the tensile properties decreases with increase in welding speed. With increase in welding speed, the heat input decreases leading to in-complete penetration thereby decrease in the tensile properties. For the same properties, heat treated weldments (Figure 8d) showed similar trend as that of the as-welded samples. However, the variation in the strength properties of heat treated samples is lower at low welding speed compared to as-welded sample. At higher welding speed, the variation in UTS is higher for heat-treated samples. The UTS values of heat-treated samples are lower at low welding speed and higher at high welding speed compered to as-welded samples. The similar observation can also be made for % EL.
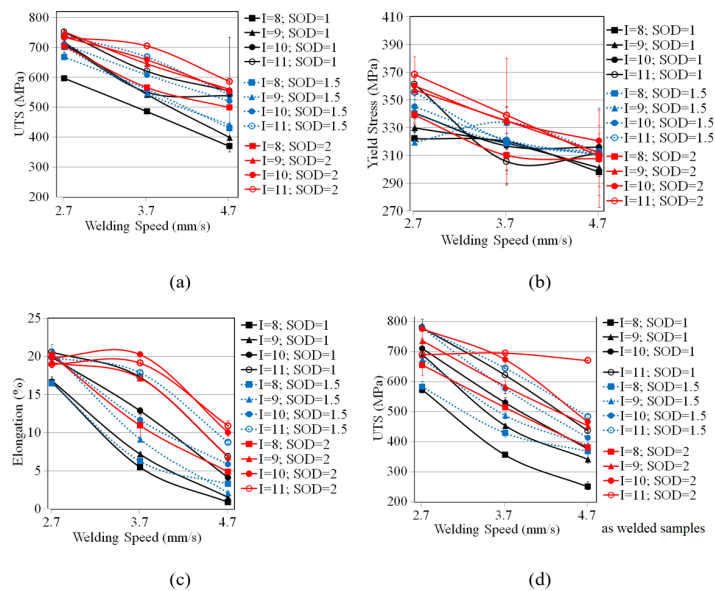
Figure 8. Variation of (a) UTS, (b) yield stress and (c) percentage elongation with welding speed of heat treated samples (d) UTS with welding speed for as-welded samples [32].

Figure 9a-c shows the plots of UTS, YS and % EL values vs. stand-off distance. Again, similar trend is observed for both heat treated and as-welded weldments (Figure 9d) for the same tensile properties. However, the variations of tensile properties of heat-treated weldments are less compared to as-welded weldments for all values of stand-off distance.
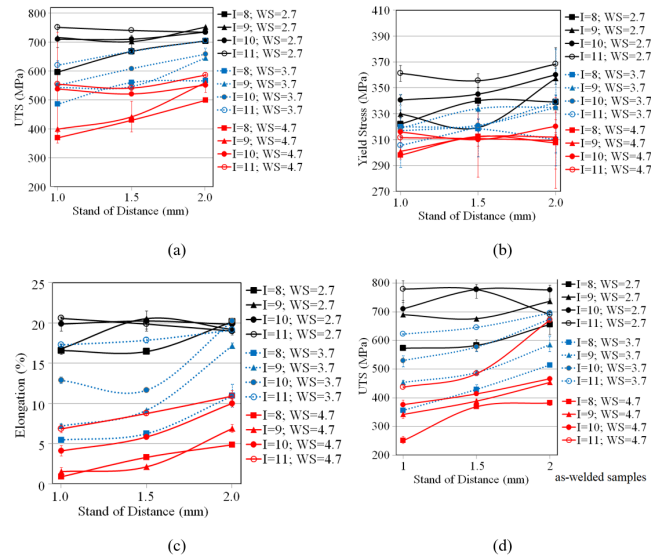
Figure 9. Variation of (a) UTS, (b) yield stress and (c) percentage elongation with stand-off distance of heat treated samples (d) UTS with stand of distance for as-welded samples [32].

3.2.3. Influence of process parameters on mechanical properties

In section 3.2.2, it was found that the variations of weld strength cannot be fully explained by individual parameters and yield strength did not show any relation with the individual process parameters. The quantitative effect of various factors and their interaction on the tensile properties of the weld is performed using three-way ANOVA. The percentage contributions of each factor and interaction on the tensile properties have been calculated and given in Table 4. It is found that the contribution of welding speed is much higher compare to all other parameters and their interaction effects. The welding current is the next most influencing factor for controlling the tensile properties. Bharatha et al. [8] also found that welding speed is the most influencing factor and next is welding current. However, the influences of individual parameters, expect welding speed, as well as the interaction effects are found insignificant for YS. The contribution of error is insignificantly and low for %EL. However, contribution of error is significantly for YS and UTS.

Table 4. Percentage influence of process parameters on weld strength.

Quality parameters	Percentage influence of welding process parameters (factors)							
	I	WS	SOD	I×SOD	I×WS	SOD×WS	I×SOD×WS	Error
UTS	13.8	61.7	6.9	#	#	#	#	17.6
Yield stress	1.3#	37.8	3#	#	#	#	#	57.9
% elongation	12.8	70.5	6.7	3.9	1.1	2.4	1.4	1.2

effect of these parameters is insignificant at 90% confidence level.

3.2.4. Development of mathematical models

The relation between the MPAW process parameters and the mechanical properties of the weld joint for heat treated samples are examined using multiple regression models. The regression models developed for UTS, YS, and percentage elongation (Elong) are as follows:

$$UTS = 701 + 83I + 16(SOD) - 336(WS) - 3.04I^2 + 42.7(SOD)^2 + 8.2(WS)^2$$
$$-16.6I(SOD) + 14.3I(WS) + 50(SOD)(WS) - 2.8I(SOD)(WS) \tag{3}$$

$$YS = 166 + 37I + 2(SOD) - 13.1(WS) - 1.12I^2 + 4.9(SOD)^2 + 5.16(WS)^2$$
$$+2I(SOD) - 3.52I(WS) - 4.2(SOD)(WS) - 0.2I(SOD)(WS) \tag{4}$$

$$Elong = -18.9 + 6.46I + 27.5(SOD) + 2.12(WS) - 0.005I^2 + 4.02(SOD)^2 - 0.6(WS)^2$$
$$-4.47I(SOD) - 0.74I(WS) - 6.99(SOD)(WS) + 0.9I(SOD)(WS) \tag{5}$$

The ANOVA test results are presented in Table 5 for UTS, YS, and %EL. From the tabulated result it is found that the regression models are adequate at 95% confidence level. The values of correlation coefficient (shown in Table 6) for the model %EL is above 0.9 and it is close to 0.9 for UTS but the R^2 values for YS model is very small. So, from the values of correlation coefficients, it can be concluded that the multiple regression model is unsuitable to represent the relationship between the selected control parameters and YS of the weld. Similar results were also found in the analysis of contribution of process parameters on the tensile properties, The R^2_{adj} values for UTS and %EL are close to ordinary R^2 values of the corresponding models. It suggests that these two models are well generalized models.

Table 5. ANOVA **table for** regression models of UTS, yield stress and percentage elongation.

Model	DOF	SOS	V	F-Value	P-Value	Whether the model is adequate
UTS	10	742929	74292.2	39.94	<0.0001	**Yes**
YS	10	19804	1980.4	6.82	<0.0001	**Yes**
%EL	10	2907.61	290.76	75.44	<0.0001	**Yes**

Table 6. The values of regression coefficient of the developed models.

Equation	R^2 value	Adjusted R^2 value
UTS (Equation 3)	86.75%	84.58%
YS (Equation 4)	53.19%	45.39%
%EL (Equation 5)	92.52%	91.29%

3.3. Analysis of micro-hardness

The variation of micro-hardness along the weld zones (i.e. various points along a layer) and across the thickness (i.e. top, middle and bottom layers) is shown in Figure 10. Figure 10a shows no significant variation in the hardness of top, middle and bottom layer of HAZ. Similarly, it is evident from Figure 10b that there is no significant variation in hardness at the right side of HAZ. Figure 10c indicates that the average hardness of left and right sides of HAZ are same. Therefore the average of all six hardness values of the HAZ is considered for analysis purpose. It is also observed (Figure 10d) that the hardness value of heat treated weldments at the HAZ increases with increase in heat input up to 65.7 J/mm. With further increase in heat input, the hardness remains almost constant at 197 HV (in the range of 182-208 HV).

Figure 11 shows the plot of hardness variation with heat input at different location (from P1 to P5 shown in Figure 1) in the fusion zone. From the figure it can be concluded that the difference in hardness values at various location of the fusion zone is marginal. The variation of average hardness at the fusion zone (Figure 11b) is showing the same trend as that in the HAZ.
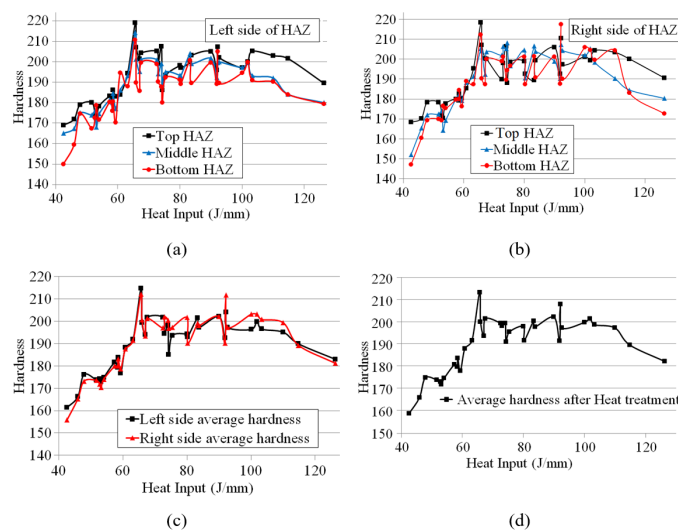
Figure 10. Variation of micro-hardness of heat treated samples with heat input in the (a) left side of HAZ (b) right side of HAZ, (c) average left and right sides and (d) average of all six points in the HAZ.
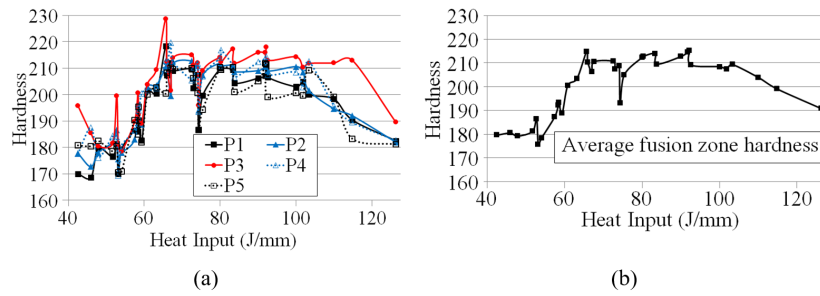
Figure 11. Hardness variation in the fusion zone of (a) all points of middle layer and (b) average of all seven points in the fusion zone.

The variation of hardness along the weld zones (*i.e.* various points along the middle layer) for both as-welded and heat treated samples is shown in Figure 12. The location 9 and location 12 are located in the left and right sides of the HAZ, respectively. The locations 1-5 are as-per Figure 1. It can be seen that the heat treated samples are having uniform micro-hardness across the various weld zones compared to the as-welded samples.
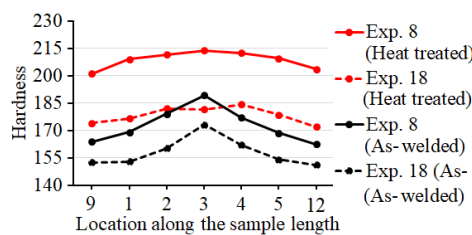
Figure 12. Micro-hardness variation along various weld zones of the middle layer for Exp. No.8 & Exp. No.18.

3.3.1. Effect of process parameters on micro-hardness

The variation in average hardness values of fusion zone and HAZ after heat treatment with process parameters are shown in Figure 13 and Figure 14, respectively. No specific trend with process parameters is observed. This due to the fact that heat treatment has reduced the harmful effect of the welding heat input. However, it appears that the process parameter also has some influence on the micro-hardness. This could be evaluated by ANOVA.
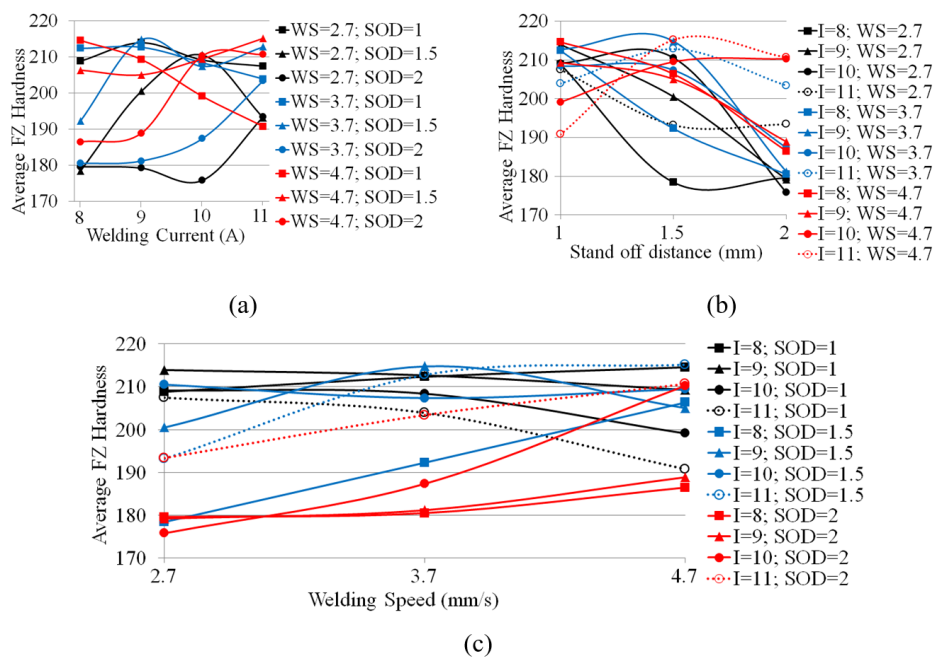
Figure 13. Variation of average fusion zone hardness with (a) welding current, (b) stand-off distance and (c) welding speed.
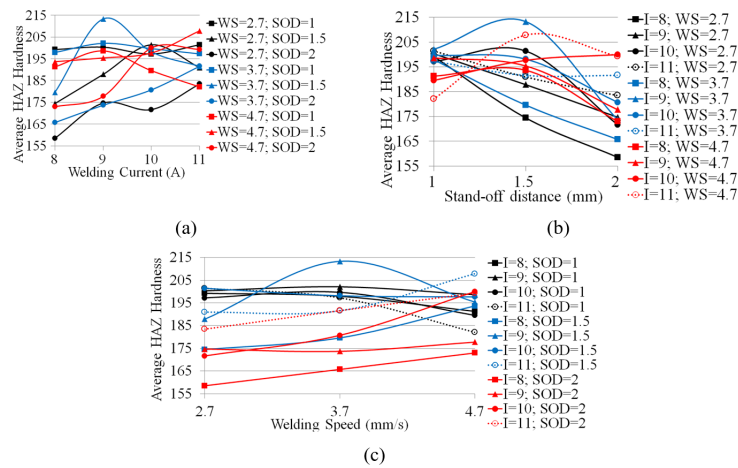
Figure 14. Variation of average HAZ hardness with (a) welding current, (b) stand-off distance and (c) welding speed.

3.3.2. Influence of process parameters on micro-hardness

Result of the ANOVA analysis is presented in Table 7. Analysis reveals stand-off distance as the most influencing factor for micro-hardness at weld cross-section. This is followed by welding current and interaction of current and stand-off distance. The error is above 10%. Welding speed appears to be the least significant parameter.

Table 7 Percentage influence of process parameters on micro-hardness of heat treated samples

	Percentage influence of welding process parameters (factors)							
	I	**WS**	**SOD**	**I×SOD**	**I×WS**	**SOD×WS**	**I×SOD×WS**	**Error**
Hardness in HAZ	14.9	2.8	37.4	13.3	–	11.5	7.9	12.2
Hardness in fusion zone	4.5	6.4	37.0	20.4	–	11.0	6.5#	14.2

effect of these parameters is insignificant at 90% confidence level

3.3.3 Development of mathematical models

The regression equation developed for the micro-hardness at HAZ and fusion zone are shown in Equations 6 and 7, respectively. The ANOVA test results are presented in Table 8. From the tabulated result it is found that the regression models are adequate at 95% confidence level. The values of correlation coefficients (shown in Table 9) for both the models are more than 0.8 indicating reasonably good co-relationship between the control parameters and micro-hardness. The models are also generalized models as adjusted R^2 values are close to the regression coefficient.

$$H_{Avg}^{HAZ} = -77 + 49.2I + 109(SOD) + 24.3(WS) - 2.25I^2 - 5.86(SOD)^2 - 6.54(WS)^2$$
$$-13.9I(SOD) - 0.3I(WS) - 20.9(SOD)(WS) + 3.5I(SOD)(WS) \tag{6}$$

$$H_{Avg}^{FZ} = -66 + 37.4I + 223(SOD) + 51.9(WS) - 0.91I^2 - 6.31(SOD)^2 - 5.19(WS)^2$$
$$-25.2I(SOD) - 4.21I(WS) - 49.4(SOD)(WS) + 6.44I(SOD)(WS) \tag{7}$$

Table 8. ANOVA **table for** regression models of average micro-hardness of HAZ and fusion zone.

Model	DOF	SOS	V	F-Value	P-Value	Whether the model is adequate
H_{Avg}^{HAZ} (Equation 6)	10	4565.46	456.55	11.51	<0.001	**Yes**
H_{Avg}^{FZ} (Equation 7)	10	4501.46	450.15	10.18	<0.001	**Yes**

Table 9. The values of regression coefficient of the developed models.

Equation	R^2 value	Adjusted R^2 value
Equation 6	82.15%	75.01%
Equation 7	80.29%	72.41%

4. Conclusion

The MPAW process offers an acceptable solution for joining most of the thin sheet materials with minimum cost. However, challenges are existent in joining SS 316L sheet using MPAW process which includes selection of suitable process parameters, desired performance level of different quality attributes, post welding heat treatment, etc. Experiments were conducted over wide range of welding current and welding speed to identify welding window for successful joining. Once the feasibility ranges of the process parameters were identified, a full factorial design matrix was developed by varying welding current, speed and SOD. In order to eliminate inhomogeneity in the mechanical and microstructural properties, the welded samples were given post welding heat treatment. The effect of heat treatment on the weld quality was investigated in details. The salient findings of the present research work are as follows:

1   Heat treatment of the weldments results in removal of HAZ thereby achieving a more homogeneous microstructure compared to as welded sample;

2   Heat treatment of the weldments results in grain coarsening at the heat affected zone. Though heat treatment results in large scatter in grain size values at low welding heat inputs, the scatter was relatively low for heat inputs greater than 83 J/mm in most of the samples;

3   Heat treatment nullifies the effect of process parameters on the grain size of the weldments. This is also confirmed by ANOVA analysis and regression model;

4   The UTS of heat treated weldments are higher than that of the as-welded samples for welding heat input up to 92 J/mm. Beyond 92 J/mm, the mechanical properties are almost similar to that of the as-welded samples. During heat treatment, the residual stresses and other metallurgical non-homogeneities were reduced resulting in higher UTS;

5   In general, there is a significant improvement in the UTS and % elongation of the weldments by heat treatment for the samples welded at low energy inputs;

6   Uniform hardness was achieved in the weld zone after heat treatment of the weldments. However, the hardness values obtained was dependent on the weld penetration which is influenced by the process parameter / welding heat input;

7   No strong correlation between weld quality and process parameters were observed after heat treatment.

References

[1]   Liu HH, Wang LB, Liu WJ, Li LY, Yue JF. Influence of AC magnetic field on the cladding layer during the microbeam plasma welding of austenitic stainless steel. International Journal of Advanced Manufacturing Technology. 2018;97(9-12):3459-3468. http://dx.doi.org/10.1007/s00170-018-2182-8.

[2]   Prasad SK, Rao CS, Rao DN. Advances in PAW: a review. Journal of Mechanical Engineering and Technology. 2012;4(1):35-59.

[3]   Desai RS, Bag S. Influence of displacement constraints in thermomechanical analysis of laser micro-spot welding process. Journal of Manufacturing Processes. 2014;16(2):264-275. http://dx.doi.org/10.1016/j.jmapro.2013.10.002.

[4]   Brien RLO. Modelling the transient heat transfer for the controlled pulse key-holing process in PAW. Vol. 2. Florida: AWS; 1991. Welding handbook, chap. 10.

[5]. Prasad SK, Rao CS, Rao DN. A study on weld quality characteristics of pulsed current micro PAW of SS304L sheets. International Transaction Journal of Engineering, Management & Applied Sciences & Technologies. 2011;437-447.

[6]   Batool S, Khan M, Jaffery SHI, Khan A, Mubashar A, Ali L, et al. Analysis of weld characteristics of microplasma arc welding and tungsten inert gas welding of thin stainless steel (304L) sheet. Journal of Materials: Design and Applications. 2016;230(6):1005-1017.

[7]   Baruah M, Bag S. Characteristic difference of thermo-mechanical behavior in plasma microwelding of steels. Welding in the World. 2017;61(4):857-871. http://dx.doi.org/10.1007/s40194-017-0472-7.

[8]   Bharath P, Sridhar VG, kumar MS. Optimization of 316 stainless steel weld joint characteristics using taguchi technique. Procedia Engineering. 2014;97:881-891. http://dx.doi.org/10.1016/j.proeng.2014.12.363.

[9]   Feng Y, Luo Z, Liu Z, Li Y, Luo Y, Huang Y. Keyhole gas tungsten arc welding of AISI 316L stainless steel. Materials & Design. 2015;85:24-31. http://dx.doi.org/10.1016/j.matdes.2015.07.011.

10.   Tam SC, Lindgren LE, Yang LJ. Computer simulation of temperature fields in mechanized PAW. Journal of Mechanical Working Technology. 1989;19:23-33.

[11] Urena A, Otero E, Utrilla MV, Munez CJ. Weldability of a 2205 duplex stainless steel using PAW. Journal of Materials Processing Technology. 2007;182(1-3):624-631. http://dx.doi.org/10.1016/j.jmatprotec.2006.08.030.

[12] Yoshioka S, Miyazaki T, Kimura T, Komatsu A, Kinoshita N. Thin-plate welding by a high-power density small diameter plasma arc. CIRP Annals. 1993;42(1):215-218. http://dx.doi.org/10.1016/S0007-8506(07)62428-7.

[13] Saha D, Pal S. Microstructure and work hardening behavior of micro-plasma arc welded AISI 316L sheet joint. Journal of Materials Engineering and Performance. 2019;28(5):2588-2599. http://dx.doi.org/10.1007/s11665-019-04064-5.

[14] Almeida DF, Martins RF, Cardoso JB. Numerical simulation of residual stresses induced by TIG butt-welding of thin plates made of AISI 316L stainless steel. Procedia Structural Integrity. 2017;5:633-639. http://dx.doi.org/10.1016/j.prostr.2017.07.032.

[15] Verma J, Taiwade RV. Dissimilar welding behavior of 22% Cr series stainless steel with 316L and its corrosion resistance in modified aggressive environment. Journal of Manufacturing Processes. 2016;24(1):1-10. http://dx.doi.org/10.1016/j.jmapro.2016.07.001.

[16] Sabzi M, Dezfuli SM. Drastic improvement in mechanical properties and weldability of 316L stainless steel weld joints by using electromagnetic vibration during GTAW process. Journal of Manufacturing Processes. 2018;33:74-85. http://dx.doi.org/10.1016/j.jmapro.2018.05.002.

[17] Kose C, Kacar R. The effect of preheat & post weld heat treatment on the laser weldability of AISI 420 martensitic stainless steel. Materials & Design. 2014;64:221-226. http://dx.doi.org/10.1016/j.matdes.2014.07.044.

[18] Liu F, Hwang YH, Nam SW. The effect of post weld heat treatment on the creep-fatigue behavior of gas tungsten arc welded 308L stainless steel. Materials Science and Engineering A. 2006;427(1-2):35-41. http://dx.doi.org/10.1016/j.msea.2006.03.105.

[19] Pandey C, Mohan Mahapatra M, Kumar P, Thakre JG, Saini N. Role of evolving microstructure on the mechanical behaviour of P92 steel welded joint in as-welded and post weld heat treated state. Journal of Materials Processing Technology. 2019;263:241-255. http://dx.doi.org/10.1016/j.jmatprotec.2018.08.032.

[20] Bal KS, Dutta Majumdar J, Roy Choudhury A. Effect of post-weld heat treatment on the tensile strength of laser beam welded Hastelloy C-276 sheets at different heat inputs. Journal of Manufacturing Processes. 2019;37:578-594. http://dx.doi.org/10.1016/j.jmapro.2018.12.019.

[21] Du C, Wang X, Luo C. Effect of post-weld heat treatment on the microstructure and mechanical properties of the 2205DSS/Q235 laser beam welding joint. Journal of Materials Processing Technology. 2019;263:138-150. http://dx.doi.org/10.1016/j.jmatprotec.2018.08.013.

[22] Xin J, Fang C, Song Y, Wei J, Xu S, Wu J. Effect of post weld heat treatment on the microstructure and mechanical properties of ITER-grade 316LN austenitic stainless steel weldments. Cryogenics. 2017;83:1-7. http://dx.doi.org/10.1016/j.cryogenics.2017.02.001.

[23] Jang D, Kim K, Kim HC, Jeon JB, Nam D-G, Sohn KY, et al. Evaluation of mechanical property for welded austenitic stainless Steel 304 by following post weld heat treatment. Korean Journal of Metals and Materials. 2017;55(9):664-670. http://dx.doi.org/10.3365/KJMM.2017.55.9.664.

[24] Barbosa Gonçalves R, Henrique Dias de Araújo P, José Villela Braga F, Augusto Hernandez Terrones L, Pinheiro da Rocha Paranhos R. Effect of conventional and alternative solution and stabilizing heat treatment on the microstructure of a 347 stainless steel welded joint. Welding International. 2017;31(3):196-205.

[25] Gonzaga AC, Barbosa C, Tavares SSM, Zeemann A, Payão JC. Influence of post welding heat treatments on sensitization of AISI 347 stainless steel welded joints. Journal of Materials Research and Technology. 2020;9(1):908-921. http://dx.doi.org/10.1016/j.jmrt.2019.11.031.

[26] Tyson W. Embrittlement of types 316l and 347 weld overlay by post-weld heat treatment and hydrogen. Metallurgical and Materials Transactions. A, Physical Metallurgy and Materials Science. 1984;15:1475-1484.

[27] Hamada I, Yamauchi K. Sensitization behavior of type 308 stainless steel weld metals after postweld heat treatment and low-temperature aging and its relation to microstructure. Metallurgical and Materials Transactions. A, Physical Metallurgy and Materials Science. 2002;33(6):1743-1754. http://dx.doi.org/10.1007/s11661-002-0183-5.

[28] ASM International. Heat treating. Vol. 4. Materials Park: ASM International; 1991.

[29] Silva CC, de Miranda HC, de Sant'Ana HB, Farias JP. Microstructure, hardness and petroleum corrosion evaluation of 316L/AWS E309MoL-16 weld metal. Materials Characterization. 2009;60(4):346-352. http://dx.doi.org/10.1016/j.matchar.2008.09.017.

[30] Sánchez-Tovar R, Montañés MT, García-Antón J. Effect of the micro-plasma arc welding technique on the microstructure and pitting corrosion of AISI 316L stainless steels in heavy LiBr brines. Corrosion Science. 2011;53(8):2598-2610. http://dx.doi.org/10.1016/j.corsci.2011.04.019.

[31] Lippold JC, Kotecki DJ. Welding metallurgy and weldability of stainless steel. USA: Wiley Student Edition; 2014.

[32] Prasad S, Pal S, Robi PS. Analysis of weld characteristics of micro plasma arc welded thin stainless steel 3 06L sheet. Journal of Manufacturing Processes. 2020;57:957-977. http://dx.doi.org/10.1016/j.jmapro.2020.07.062.

[33] Montgomery DC. Design and analysis of experiments. 8th ed. USA: Wiley Student Edition; 2013.